Mahmut A. Ermeydan | Etienne Cabane | Philipp Hass
Joachim Koetz | Ingo Burgert

Fully biodegradable modification of wood for improvement of dimensional stability and water absorption properties by poly(ε-caprolactone) grafting into the cell walls

Suggested citation referring to the original publication:
Green Chem. 16 (2014), pp. 3313–3321
DOI http://dx.doi.org/10.1039/c4gc00194j

Green Chemistry

PAPER

View Article Online
View Journal | View Issue

Cite this: *Green Chem.*, 2014, **16**, 3313

Fully biodegradable modification of wood for improvement of dimensional stability and water absorption properties by poly(ε-caprolactone) grafting into the cell walls†

Mahmut A. Ermeydan,[a,b,c] Etienne Cabane,[a,b] Philipp Hass,[a,b] Joachim Koetz[d] and Ingo Burgert*[a,b]

Received 5th February 2014,
Accepted 15th April 2014

DOI: 10.1039/c4gc00194j

www.rsc.org/greenchem

Materials derived from renewable resources are highly desirable in view of more sustainable manufacturing. Among the available natural materials, wood is one of the key candidates, because of its excellent mechanical properties. However, wood and wood-based materials in engineering applications suffer from various restraints, such as dimensional instability upon humidity changes. Several wood modification treatments increase water repellence, but the insertion of hydrophobic polymers can result in a composite material which cannot be considered as renewable anymore. In this study, we report on the grafting of the fully biodegradable poly(ε-caprolactone) (PCL) inside the wood cell walls by $Sn(Oct)_2$ catalysed ring-opening polymerization (ROP). The presence of polyester chains within the wood cell wall structure is monitored by confocal Raman imaging and spectroscopy as well as scanning electron microscopy. Physical tests reveal that the modified wood is more hydrophobic due to the bulking of the cell wall structure with the polyester chains, which results in a novel fully biodegradable wood material with improved dimensional stability.

Introduction

Wood has been known and used as a renewable raw and engineering material for thousands of years and is still nowadays an essential building material due to desirable features such as light weight, processability, good mechanical properties, sustainability, and aesthetic appearance.[1–3] A further strong argument in view of the development towards more sustainable societies is that wood is suitable for energetic recovery at the end of its service time, after an ideally long-lasting carbon storage in a high value application.

However, wood has some drawbacks, related to the cell wall hydrophilic nature, which limit its long term usage as an engineering material. Wood cell walls are composed of longitudinally oriented cellulose fibrils embedded within an amorphous hemicellulose and lignin matrix,[4] and as such, they can absorb large amounts of water from the environment. Water absorption and desorption cycles due to humidity changes cause swelling and shrinking of the cell walls, leading to dimensional instability that can result in severe deformation or crack initiation and failure of the wood material.[1–3] In addition, the presence of water in the cell wall provides an appropriate environment for fungal attack resulting in the biodegradation of wood.[1,3,5]

Research in the field of wood modification focuses mainly on decreasing the water uptake of cell walls, in order to increase wood dimensional stability. It is well known that chemicals have to penetrate into the cell wall structure and have to be locked inside in order to have a strong impact on wood properties.[1,3,6] As an example, the formation of covalent bonds between –OH groups of cell wall polymers and small reactive molecules is a well-documented approach.[7–9] Another option is *in situ* grafting polymerization of monomers.[1,3,10] Various challenges have to be considered when modifying wood cell walls, for example, the use of mild conditions to avoid degradation of the cell wall structure during modification reactions, or the elimination of harmful by-products. In addition, the hygroscopic nature of the cell walls is a severe barrier to the introduction of hydrophobic materials, and impedes the insertion of small molecules solubilized in polar solvents. There are several studies on *in situ* polymerization of

[a]*ETH Zurich, Institute for Building Materials, Zurich, Switzerland. E-mail: iburgert@ethz.ch*
[b]*Empa – Swiss Federal Laboratories for Material Testing and Research, Applied Wood Research Laboratory, Dübendorf, Switzerland*
[c]*Max Planck Institute of Colloids and Interfaces, Department of Biomaterials, Potsdam, Germany*
[d]*University of Potsdam, Institute of Chemistry, Potsdam, Germany*
† Electronic supplementary information (ESI) available: Additional data and graphics, methods. See DOI: 10.1039/c4gc00194j

hydrophobic monomers inside wood, but very few of them report on the successful insertion of polymers inside the cell wall structure, and as a result, on an efficient improvement of dimensional stability.[11–15] Recently, our group reported on a wood pre-treatment enhancing the introduction of hydrophobic molecules within the cell wall.[16] We successfully inserted hydrophobic flavonoid molecules inside the cell walls, yielding a wood material with reduced water uptake as well as increased dimensional stability.

In addition to the research on improving wood properties, the development of novel wood based engineering materials is also driven by ecological concerns (sustainability, eco-efficiency, and recyclability of the products). In the field of wood modification with synthetic polymers, the commonly used chemicals yield wood-polymer composite materials that have to be considered as plastics when it comes to recycling.[17] To overcome this drawback, it is preferable to utilize biodegradable polymers for modification and develop waste-free materials.[18] The main strategies to eliminate the disposal problem of materials are the utilization of polymeric materials derived from renewable resources (*e.g.* wood flour, starch, cellulose, and chitin) and the production of composites with biodegradable synthetic materials (such as polyesters including poly(ε-caprolactone), poly(lactic acid), poly(3-hydroxybutyrate), and poly(glycolic acid)).[18–22] Poly(ε-caprolactone) (PCL) is one of the most widely evaluated and systematically studied biodegradable synthetic polymers.[18,19] It is a semi-crystalline hydrophobic polyester that can be polymerized by ring opening polymerization initiated by alcohols. The combination of PCL with wood derived products has been investigated previously, mainly for the development of biodegradable materials based on wood particles or components (such as wood flour and PCL blends, or grafting of caprolactone from cellulose).[23–25]

In view of the abovementioned advantages of PCL, we regarded caprolactone as an interesting candidate for *in situ* polymerization of wood and we report here on the first attempt to graft solid wood with poly(caprolactone) chains. For that purpose, we prepared a fully biodegradable material obtained by the ROP of caprolactone monomer initiated by –OH groups from cell wall components. Dimensional stability and water repellence of the modified wood are significantly improved, while the natural attributes of wood are retained, which shows that the new material can potentially be used as a fully green material.

Experimental

Materials

ε-Caprolactone (CL), tin(II) 2-ethylhexanoate ($Sn(oct)_2$), dry dimethyl formamide (DMF), dry toluene, and acetone were bought from Sigma-Aldrich and used as received.

Chemical modification of wood cubes

Wood sampling. Sixty Norway spruce (*Picea abies*) sapwood cubes (1 cm × 1 cm × 0.5 cm; radial × tangential × longitudinal, respectively) were cut along the grain, and dried in an oven at 63 °C overnight. The cubes were divided into four sets of fifteen cubes: one set as reference wood (*i.e.* untreated), one set as controls (*i.e.* placed under the reaction conditions without the reactive compounds), and two sets for full modification. After treatment, ten cubes from each set were used for physical characterization (*i.e.* leaching, swelling (S), water uptake (WU), anti-swelling efficiency (ASE) tests, equilibrium moisture content (EMC), and contact angle measurement). The rest of the cubes were used for structural, chemical, and mechanical analysis. A detailed description of the experimental workflow is given in ESI (Fig. S1†), and the reaction scheme and sample nomenclature are summarized in Fig. 1.

Impregnation and *in situ* ring opening polymerization of PCL. The wood cubes were dried at 63 °C for one day to reach a nearly dry wood cube with estimated moisture content around 1%. Cubes were placed in 50 ml of anhydrous DMF or toluene. After one day of swelling, the cubes were placed in flasks containing a solution of ε-caprolactone (20 g) with 2% (w/w) of $Sn(Oct)_2$ as the initiator. The cubes were stored in this solution for one day in order to maximize monomer impregnation in wood cell walls before polymerization. Prior to the

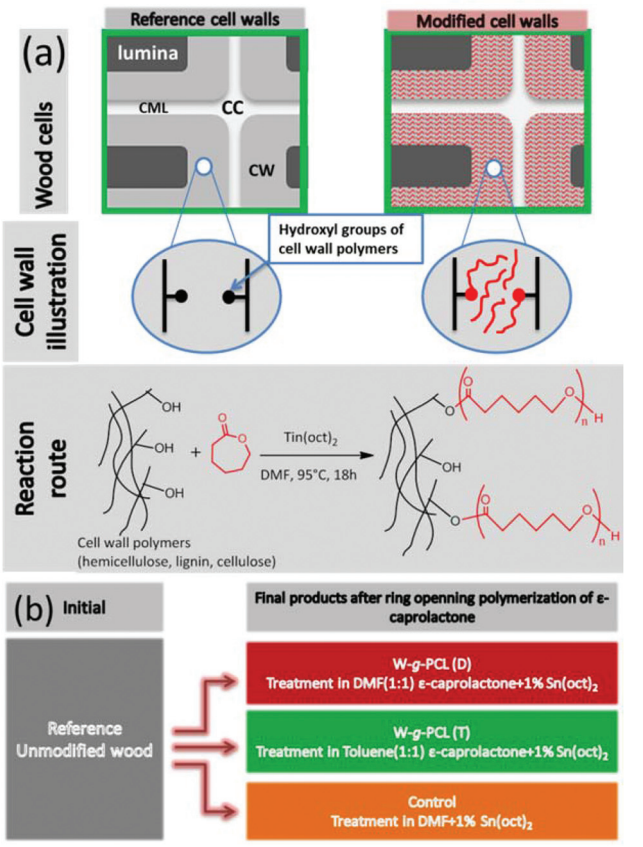

Fig. 1 (a) Schematic illustration and reaction route of polycaprolactone grafting on the cell wall polymers (CML: compound middle lamella, CC: cell corner, CW: cell wall). (b) Nomenclature for the treatment of spruce wood blocks under different conditions.

reaction, 20 ml of dry DMF or toluene were added to the flask and the solution was degassed by bubbling argon for 30 minutes. The reaction flasks were heated to 95 °C for 18 hours to polymerize ε-caprolactone. After reaction completion, the wood cubes were washed with several volumes of acetone (approx. 4 hours), then with water (24 hours), and finally dried in the oven at 63 °C for 24 hours. Additional acetone washing was carried out by Soxhlet extraction for 96 hours to estimate how much polycaprolactone is chemically grafted on cell wall polymers. All solvents used for polymerization reactions and washing steps (DMF, toluene, acetone) are good solvents for both the ε-caprolactone monomer and the poly(caprolactone) polymer.

Characterization

Raman spectroscopy and imaging. 30 μm thick cross-sections were cut on a rotary microtome (LEICA RM2255, Germany) in a region 0.5–1 mm below the surface of the wood cubes and placed between the glass microscope slide and the coverslip with a drop of water to maintain cell walls under wet conditions. Spectra were acquired with a confocal Raman microscope (alpha300, WITec GmbH, Ulm, Germany) equipped with an objective (60×, NA = 0.8, 0.17 mm coverslip correction from Nikon Instruments, Amstelveen, The Netherlands). A 532 nm laser (Crysta Laser, Reno, NV, USA) was focused with a diffraction limited spot size of 0.61 λ/NA and the Raman signal was detected with an air cooled back illuminated CCD camera (DV401-BV, Andor, Belfast, North Ireland) behind the spectrograph (UHTS 300, WITec) with a spectral resolution of 3 cm^{-1}. For mapping, an integration time of 0.4 s was chosen, and every pixel corresponds to one spectrum acquired every 0.5 μm. Two-dimensional chemical images of the wood components and added polyester were compiled using WitecProject software with the integration filter.

Scanning electron microscopy (SEM) and energy dispersive X-ray (EDX) analysis. Structural details of the treated and untreated wood samples were analysed using an (E)SEM device (FEI FEG-ESEM Quanta 600, FEI Company, Hillsboro, OR, USA) with a backscattered electron (BSE) detector operated at 7.5 kV with a 10 mm sample–detector distance, 4.0 nm spot size, and 0.75 Torr pressure. EDX analysis was performed using the INCA Energy 300 system (Oxford Instruments, UK) with an X-Max 80-Detector. Samples were coated with platinum before analysis.

Volume change and weight percentage gain (WPG). Dimensions and weights of the wood cubes were measured before and after all treatments (polymerization, water immersion, and drying) in order to determine the volume and weight changes caused by the chemical treatment.

Swelling coefficient (S), anti-swelling efficiency (ASE), and water uptake (WU). The reference, control and treated cubes were immersed in deionized water for five days with moderate shaking (soak cycle 1). Then cubes were placed in an oven at 103 °C overnight for drying (drying cycle 1). Samples were immersed again in deionized water for the second water-soaking and subsequent drying cycles. The degree of dimensional stability of the modified wood cubes was obtained by calculating the S and the ASE as reported.[26] The equations for swelling, anti-swelling efficiency, and WU calculations are given in ESI (Fig. S2†). The water repellence is given by the WU calculations.

Equilibrium moisture content (EMC). Wood exposed to a constant relative humidity with a constant temperature absorbs or releases water and reaches a constant moisture content called the EMC. Reference, control, and PCL-grafted samples were equilibrated in a sealed system with a relative humidity of 75% (obtained with a saturated solution of NaCl) at room temperature. When the samples reached equilibrium (*i.e.* constant weight), samples were oven-dried at 103 °C and weight differences were calculated to determine the final moisture content. For each set, five samples were used for the measurements. The equation for the EMC calculation is given in the ESI (Fig. S3†).

Contact angle measurements. Contact angle measurements were performed on a cross-section (RT-plane) of five samples per set (reference, control, W-g-PCL(D), and W-g-PCL(T)). All samples are acclimatized in normal climate (20 °C and 65% relative humidity) until equilibrium. To avoid any surface aging effects on the measurement, the cross-section was smoothened with a sledge microtome GSL 1 (WSL, Birmensdorf, Switzerland) less than 24 h before the measurement. A standard contact angle measuring device (SCA 20, dataphysics) was used to apply 11 μl droplets of distilled water (LiChrosolv®) on the smoothened cross-section and to record its evolution by taking images with an appropriate frame rate, which lay between 0.5 and 25 frames per second. Besides the comparison of the different treatments with the untreated wood samples, the procedure was repeated on plastic sheets to estimate the amount of water evaporated during the experiment. The determination of the contact angles was done using the software included in the SCA20 contact angle measuring device. For the comparison of the different surfaces, the evolution of the contact angle was fitted using a linear function and its first parameter (climax) was used. When possible, the fitting procedure started after the droplet was stabilized on the surface.

Nanoindentation. The mechanical characterization of tracheid cell walls was carried out as reported elsewhere,[16] on a Hysitron Triboscan UBI-1 nanoindentation system (Minneapolis, MN). For this purpose, samples were dried overnight at 63 °C and subsequently embedded in AGAR resin (AGAR low viscosity resin kit, AGAR Scientific Ltd, Stansted, UK). Specimens were immersed into the embedding resin and cured overnight at 60 °C. 2 mm thick slices were cut from the resin blocks. The embedded specimens were glued onto metal discs (15 mm AFM specimen discs). Surfaces were smoothed by polishing. Quasi-static indentation tests were performed in a force-controlled mode, the indenter tip (Berkovich-type triangular pyramid) was loaded to a peak force of 250 μN at a loading rate of 100 μN s^{-1}, held at constant load for 15 s, and unloaded at a rate of 100 μN s^{-1}.

Results and discussion

Poly(caprolactone) grafting inside the cell walls

Poly(caprolactone) can be prepared by catalyzed ring-opening polymerization of ε-caprolactone, mainly using metal based catalysts (poor metals such as aluminum and tin based catalysts, alkaline earth metals, transition metals, and rare earth metals),[27–30] but also enzymatic or organic catalytic systems.[31] The hydroxyl groups present in the reaction media act as co-initiators, and the polymerization proceeds through the activated stannous alkoxide species formed *in situ*.[32,33] The –OH groups of carbohydrates (such as cellulose) were already used as initiators for the ROP of caprolactone, yielding cellulose grafted with PCL chains.[34–38] Within wood, our aim was to use the abundant –OH groups present on the cell wall polymers (cellulose, lignin, and hemicellulose) to initiate the polymerization of ε-caprolactone and obtain wood grafted with polyester chains. The penetration of caprolactone in the cell wall structure is a critical step in the modification. As reported in the literature, a preferred solvent for the ε-caprolactone ROP is toluene.[30,39,40] However, it is known that the wood swelling potential of toluene is limited in comparison to DMF, which swells wood to a greater extent.[41] Since ROP of caprolactone was reported to take place in different solvents, including DMF,[42] we ran the experiments with both solvents (W-g-PCL(D) for DMF and W-g-PCL(T) for toluene). One set of wood cubes was placed in the same reaction conditions as the experiment W-g-PCL(D), but without the monomer. These samples (control(DMF)) were used for comparison with the fully treated samples. The WPG and dimensional changes resulting from the different treatments are summarized in Table 1.

The weight percent gain (WPG %) and volume change which were determined after ring opening polymerization provide a first indication of the success of the modification. W-g-PCL(D) showed the highest WPG and permanent volume change after polymer modification. The positive dimensional changes of W-g-PCL(D) and W-g-PCL(T) samples can be related to the presence of polymers within the wood cell wall: it has been shown already that a permanent volume change after a successful modification is mainly due to cell wall bulking with new material.[43,44] The values in Table 1 reported for control samples indicate a slight weight loss and a permanent volume reduction of about 7%. These observations may be explained by the leaching of some cell wall components, mainly extractives, and the DMF treatment resulted in a re-organization of the cell wall polymers (especially in the amorphous lignin/hemicellulose matrix). The WPG reduction after additional acetone washing by Soxhlet extraction reveals that homopolymers that were not attached to the cell wall polymers were removed which also resulted in a reduction of the cell wall bulking effect.

Residual tin was determined after the first washing step and was found in small amounts with a homogeneous distribution across the cell wall by EDX analysis (estimation based on EDX calculation: ~1% (w/w)) (Fig. S4†).

Table 1 Summary of weight percent gains and volume changes of spruce wood cubes after ring opening polymerization reactions with DMF and toluene, and control conditions: after initial washing and Soxhlet extraction

	Initial washing		Soxhlet extraction	
Exp. ID	WPG (%)	Vol. change (%)	WPG (%)	Vol. change (%)
W-g-PCL(DMF)	17.9	5.5	11.2	3.6
W-g-PCL(toluene)	11.2	2.4	5.2	1.8
Control(DMF)	−1.1	−7.3	N/A	N/A

Distribution of polymer in wood

To determine the spatial distribution of poly(caprolactone) after polymer modification at the cell and tissue levels, a series of SEM pictures of cube cross sections was performed. SEM images of unmodified reference cell walls are shown in Fig. 2a and b. Fig. 2c and d show that no noticeable cell wall deformations were observed for the control, which indicates that the modification process in DMF did not affect the wood tissue microstructure.

During the reaction process, wood cubes were completely immersed in the reaction solution, and it is highly expected that polymerization takes place also in the cell lumina due to trace amounts of water molecules in the solution, which can compete with cell wall –OH groups for the initiation of caprolactone ROP. However, the PCL free chains in solution were washed away with acetone after modification, and as a result, Fig. 2e and f reveal that the cell wall lumina are essentially empty for the W-g-PCL(D) samples. This result indicates that the weight gain of W-g-PCL(D) samples is mostly due to polymer bulking in the cell walls.

Although the samples modified in toluene (W-g-PCL(T)) were submitted to the same washing steps, some unbound polymer chains remain in the cell lumina and completely fill the micropores in the latewood regions (Fig. 2g and h). This might be due to differences in the solvent system which affect the degree of polymerization. Toluene is one of the most favourable solvents for efficient ε-caprolactone polymerizations under homogeneous conditions, which results in a high degree of polymerization.[45] However, toluene has limited wood swelling capabilities, which hinders the penetration of monomer into the cell wall, and therefore, one observes only little polymer in the cell wall, and some lumen filling with high molecular weight chains, when toluene is used as a solvent. In contrast, it is reported that ε-caprolactone polymerization with metal initiators in DMF can hinder the polymerization,[46] which may lead to shorter polymer chains that can in turn be more easily washed away and thus explain the absence of polyester in the cell lumina. Additionally, the excellent swelling properties of DMF allow for a more widespread polymerization inside the cell wall.

In addition to SEM analysis, we investigated chemical changes in the modified spruce cell wall structure to determine whether poly(caprolactone) was polymerized within the cell walls. In this regard, confocal Raman microscopy is a

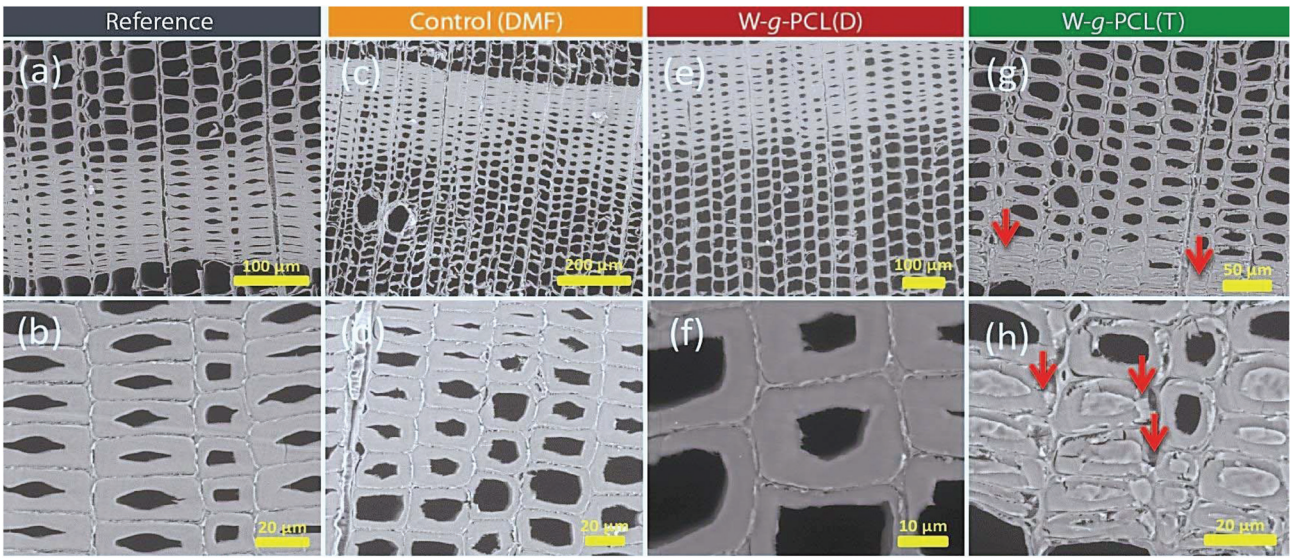

Fig. 2 SEM images of microtomed cross-sections: (a–b) untreated cell walls; (c–d) control cell walls (*i.e.* treated with DMF + $Sn(oct)_2$ at 95 °C); (e–f) *in situ* polycaprolactone grafted cell walls in DMF, and (g–h) *in situ* polycaprolactone grafted cell walls in toluene.

powerful technique for the detailed analysis of plant cell walls which provides spectroscopic analysis of cell wall constituents and can be used to construct chemical imaging of the desired components.[47–49]

Typical Raman spectra of W-g-PCL(D), W-g-PCL(T), reference, and poly(caprolactone) polymer are shown in Fig. 3. The spectra recorded for polymer grafted cell walls display the specific wood bands.[48,50]

In addition to the wood Raman bands, important changes were observed in the 1400–1500 cm^{-1} and 1700–1750 cm^{-1} regions. As shown in Fig. 3, poly(caprolactone) has strong bands between 1400 and 1500 cm^{-1} which belong to $\delta(CH_2)$ vibrations and a strong band at 1725 cm^{-1} which belongs to $\nu(C{=}O)$ vibration.[51] In the Raman spectra of polymer grafted cell walls, we observed a clear signal related to the presence of $-CH_2-$ groups from PCL. In addition, the C=O bond of the polyester can be easily visualized after modification. From the intensity distribution of the new peaks, it is clear that the modification in DMF resulted in higher PCL cell wall contents. These polyester peaks were clearly absent in the reference wood samples. In the Raman spectrum shown in Fig. 3, the Raman bands of ε-caprolactone monomer at 695 and 735 cm^{-1} (assigned to breathing motion vibrations in the seven member ring structure) cannot be found, which indicates that the modified cell walls contain only polymerized caprolactone.

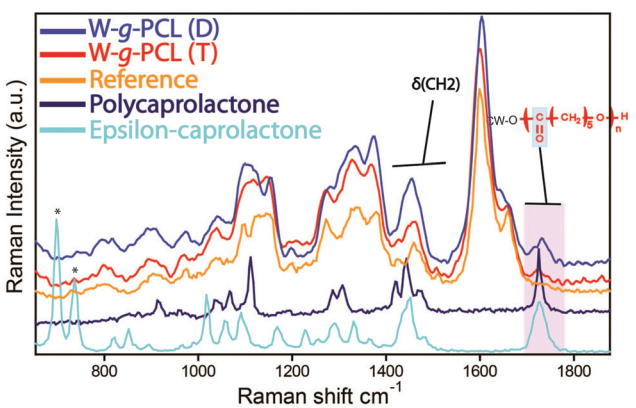

Fig. 3 Raman spectrum of poly(caprolactone) grafted cell walls [W-g-PCL(D), W-g-PCL(T)] compared with the reference, poly(caprolactone) and epsilon-caprolactone spectra in the 600–1900 cm^{-1} spectral range.

The Raman images shown in Fig. 4 were obtained *via* scanning of a latewood cross-section from poly(caprolactone) grafted cell walls, and integration of the relevant peaks for wood constituents and poly(caprolactone) found in the spectra (see characterization). In Fig. 4, images a and d represent the CH groups (from cellulose) and the lignin distributions are shown in images b and e, depicting the overall cell wall structure. The distribution of cellulose highlights the secondary cell wall regions (bright turquoise zones), whereas the lignin has higher intensity in the cell corners and compound middle lamella (bright yellow zones). The poly(caprolactone) distribution of polymer grafted cell walls (W-g-PCL(D) in Fig. 4c, W-g-PCL(T) in Fig. 4f) indicates that polymerization took place in the cell walls for both experiments (green zones). In the W-g-PCL(D) cell walls, the poly(caprolactone) polymers are rather homogeneously distributed across almost the whole secondary cell wall, in contrast to the toluene experiment W-g-PCL(T), where poly(caprolactone) is predominantly located in a cell wall region close to the lumen. In both cases, brighter regions represent higher intensity of the related components, and the images clearly show that the penetration of the monomer (consequently the polymer) inside the cell wall is more efficient when a good solvent for wood such as DMF is used.

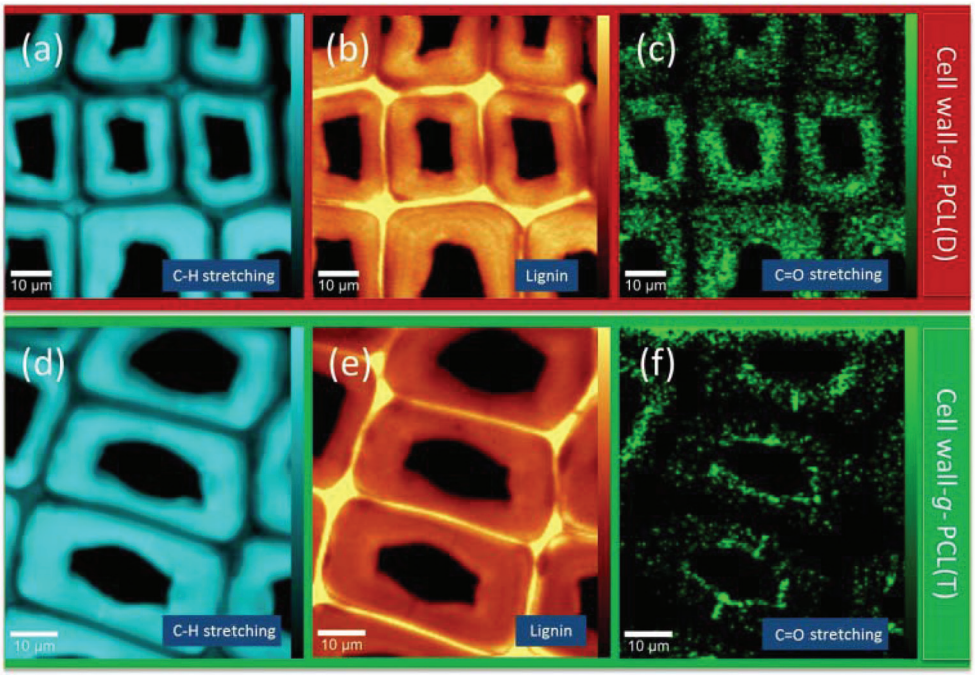

Fig. 4 Raman images (a–c: 70 × 70 µm^2 and d–f: 60 × 70 µm^2) of the latewood cell wall tissue. Images were plotted by integration of Raman bands from the spectral data set: (a, d) C–H stretching groups (mainly cellulose) (2850–3010 cm^{-1}), (b, e) lignin (1555–1660 cm^{-1}), and (c, f) polycaprolactone carbonyl group (1715–1735 cm^{-1}).

Improved wood properties

To evaluate improvements in dimensional stability and WU (water uptake) behaviour of the polyester grafted wood, we used the water-soaking method developed by Rowell *et al.*[26] This method based on subsequent cycles of drying and wetting is a common measurement protocol to assess the efficiency of wood modification treatments by the determination of changes in WU and dimensional stability as a response to water sorption/desorption.

Stability of polymers in wood and water repellence

Wood eventually loses weight during repeated soaking–drying cycles due to the removal of extractives and non-bound modifying compounds. The mass losses recorded for the different samples are given in Fig. 5a. The significant difference between the mass loss of reference wood and treated samples may be explained as follows: the untreated wood loses extractives during the soaking–drying cycles, but for the other samples, those substances were most likely removed during the various modification steps. Samples containing poly(caprolactone) (W-g-PCL(D) and W-g-PCL(T)) show only little weight loss, indicating that the added material in the modified wood is locked within the wood structure. The increase in weight loss of W-g-PCL(D) during the second cycle may be explained by removal of the shorter polymer chains from the cell lumen.

The WU ability of the samples (after the first and second water immersion cycles) is shown in Fig. 5b. After five days in

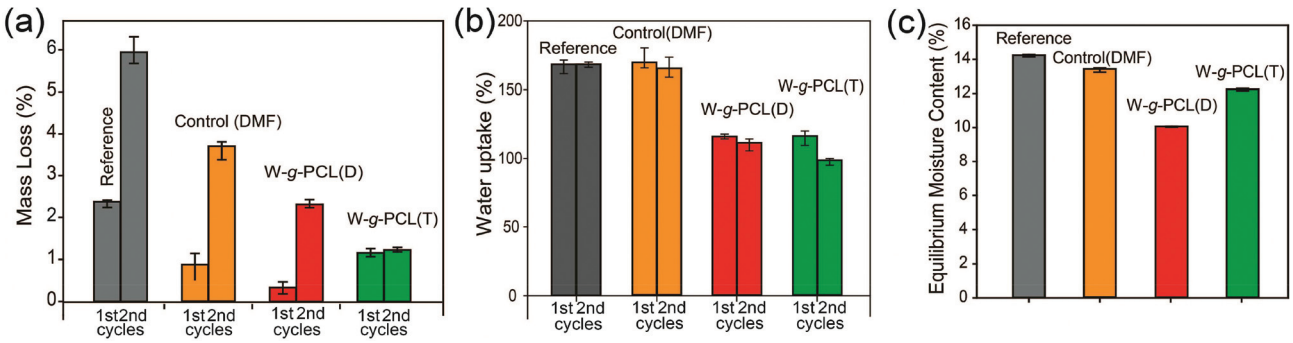

Fig. 5 (a) Determination of cumulative mass loss due to leaching of unbound material after the cubes were immersed for five days in water (1st cycle) and after another five days of immersion in water (2nd cycle). (b) WU values for reference wood, polymerized wood (W-g-PCL(D), W-g-PCL(T)), and control(DMF). (c) EMC results at 75% relative humidity for reference wood, polymerized wood (W-g-PCL(D), W-g-PCL(T)), and control (DMF).

water (1st cycle), the unmodified (reference) wood sample gains about 160% water, while wood-PCL composites gain about 100%. The trend is similar after the second immersion period. As expected, the grafted hydrophobic poly(caprolactone) chains provide some degree of protection against water uptake: the treated samples in DMF show at least 30% reduction in WU when compared to unmodified wood.

Another way to evaluate the affinity of the wood samples for water is to calculate the EMC. In this case, the samples were placed in a climate chamber with standard temperature (20 °C) and a relative humidity of 75%, to examine the WU exclusively at the cell wall level. Under these conditions, reference (unmodified) wood has an EMC of about 14%, as shown in Fig. 5c. This value is slightly lower than literature values reported for Norway spruce (14.4%), and can be explained by the natural variability of wood.[52] The polymer grafted samples show less moisture adsorption. The highest hydrophobization is shown for the W-g-PCL(D) samples with an EMC of about 10%, which represents a 30% reduction of moisture content when compared to reference samples, and correlates well with the WU experiment.

Dimensional stability of polymer grafted wood

In order to evaluate the improvement of dimensional stability of modified wood, we observed the swelling and shrinkage behaviour of the wood cubes upon water soaking–drying cycles. Calculations of volumetric S and ASE were made according to the equations given in ESI (Fig. S2†). The volumetric S values of the polymer grafted samples (W-g-PCL(D) and W-g-PCL(T)) were compared with the reference (unmodified) and control (DMF) samples after each water-soaking and drying cycle (Fig. 6).

The wood volume changes upon water soaking and drying cycles are a result of swelling and shrinking of the wood cell walls. The volume of native wood typically swells 15 to 20%, depending on species, tissue type and environmental conditions. When hydrophobic material bulks the cell wall, the water affinity for wood is decreased, and less space is available for the water molecules to enter the cell wall, resulting in decreased swelling. A lower swelling value corresponds to a higher dimensional stability. As shown in Fig. 6, the swelling of the W-g-PCL(D) samples is reduced to about 8%, while the reference wood samples swell to about 16%.

The ASE compares the swelling of unmodified wood with the swelling of treated wood. A high ASE value corresponds to high dimensional stability (see Fig. S2† for equations). The negative ASE of control samples may be explained by the removal of extractives and the re-arrangement of cell wall polymers (lignin/hemicelluloses), both phenomena contributing to a better water penetration in wood, and hence enhanced swelling. In contrast, the ASE values observed for W-g-PCL(D) samples, with values above 40% after each water immersion and drying cycle, indicate that the treatment strongly increases the dimensional stability of wood. The lower ASE values observed for the W-g-PCL(T) samples can be directly correlated with the amount of PCL located in the cell wall shown in Fig. 4c–f, and confirm that the choice of solvent for the modification largely influences the final polymer content in the cell wall.

Contact angle measurements

The bulk wood modification also results in new surface properties. In Fig. 7, we show representative curves for the evolution of the contact angle on different surfaces. The evolution of the contact angle on a plastic sheet (for comparison), the W-g-PCL(T), and W-g-PCL(D) treated surfaces fit to the applied linear function. The untreated and DMF treated surfaces absorbed the water droplet in less than 2 s and less than 0.5 s, respectively. Due to the lack of droplet stabilization, the fitting was performed using all available data points. The fast water absorption in the control samples is also reflected in the mean values for the contact angle changes which was about six times faster after the pure DMF treatment (mean climax reference: $-62.45°\ s^{-1}$; control: $-374.7°\ s^{-1}$). The comparison of the curves shows that both modification methods increase the hydrophobicity of the wood surface. After the W-g-PCL(D) treatment the contact angle decreased about 200 times more slowly than without the treatment (W-g-PCL(D): $-0.335°\ s^{-1}$). Although the total weight percent gain was higher for the modification with DMF and the spatial distribution showed a higher concentration in the cell wall for this method, the modification with toluene (W-g-PCL(T)) even led to a contact angle decrease that was again 10 times slower than that for W-g-PCL(D) (climax W-g-PCL(T): $-0.034°\ s^{-1}$). Since the

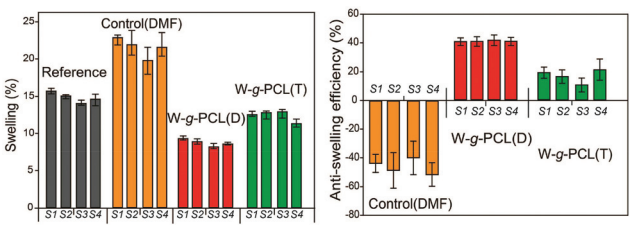

Fig. 6 Left: average volume swelling values from the immersion and drying cycles. Right: ASE values for treated wood cubes (W-g-PCL(D), W-g-PCL(T), control(DMF)).

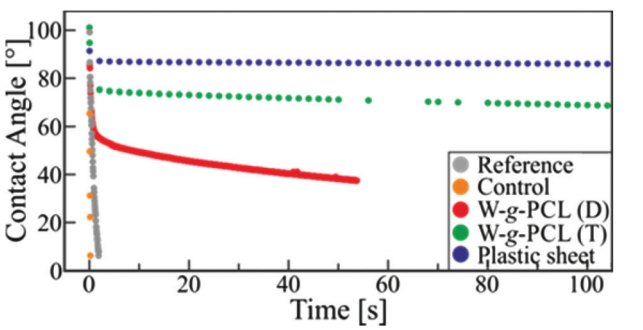

Fig. 7 Contact angle measurements of reference, control(DMF), W-g-PCL(D), W-g-PCL(T), and plastic sheet.

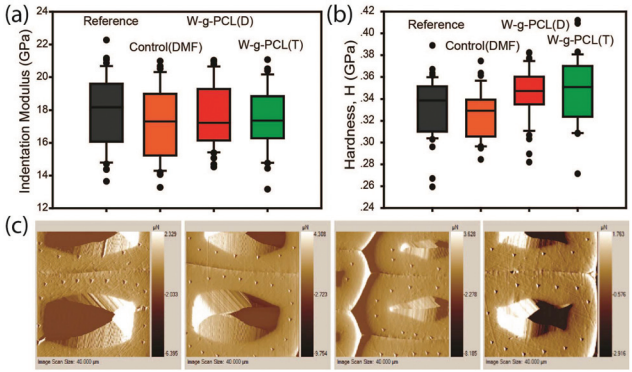

Fig. 8 (a) Indentation modulus and (b) hardness of reference, poly-caprolactone grafted, and DMF treated cell walls. (c) SPM (Scanning Probe Microscopy) images of nano-indented cell walls. Left-to-right: reference, control(DMF), W-g-PCL(D), W-g-PCL(T).

measurements were performed on cross sections with cut open cells, this behavior is probably due to the partially filled cell lumina, as was seen in Fig. 2, which was not visible for W-g-PCL(D). However, the comparison with the plastic sheet ($-0.0097°\ s^{-1}$) shows that there is still a considerable amount of water that is absorbed into the wood substrate.

Nanomechanical properties of cell walls

The mechanical properties of reference, control(DMF) and poly(caprolactone) grafted cell walls were investigated by nano-indentation (Fig. 8). The indentation modulus of modified cell walls and references were not significantly different ($P \geq 0.05$, *U*-test). PCL grafted cell walls show a slight ($P < 0.05$, *U*-test) increase in hardness when compared to the unmodified cell walls. The nanoindentation analysis essentially shows that the modification did not alter the mechanical properties of the cell walls.

Conclusions

We reported here a first attempt at grafting of polyesters within wood cell walls. The hydroxyl functionalities present in cell wall polymers were used to initiate the ring opening polymerization of caprolactone. Based on the solvent utilized in the process, different amounts of polymer could be introduced in the cell wall, yielding materials with different properties. The wood samples modified in DMF show the most significant improvements, both in terms of hydrophobic properties and dimensional stability, and this without altering the mechanical properties of the wood. Using a fully biodegradable synthetic polymer like poly(caprolactone), we were able to produce a novel wood product with improved performance, while preserving the advantage of an environmentally friendly material, which can be easily disposed or is eligible for energetic recovery. Since a wider utilization of wood-based materials is often hindered by intrinsic drawbacks and/or recycling issues, we believe that this new approach will help in enhancing the implementation of wood in given and novel applications.

Acknowledgements

We thank the Bundesamt für Umwelt (BAFU) and Lignum, Switzerland as well as the Max Planck Society, Germany for financial support. The study is embedded in the SNF NRP66 project: Improved wood materials for structures.

Notes and references

1 R. M. Rowell, *Handbook of wood chemistry and wood composites*, CRC Press, Boca Raton, FL, 2005.
2 D. Fengel and G. Wegener, *Wood: chemistry, ultrastructure, reactions*, ed. W. de Gruyter, Berlin, New York, 1984.
3 C. A. S. Hill, *Wood modification: chemical, thermal and other processes*, John Wiley & Sons, Chichester, England, Hoboken, NJ, 2006.
4 L. J. Gibson, *J. R. Soc. Interface*, 2012, **9**, 2749–2766.
5 A. Schirp and M. P. Wolcott, *Wood Fiber Sci.*, 2005, **37**, 643–652.
6 T. Furuno, Y. Imamura and H. Kajita, *Wood Sci. Technol.*, 2004, **37**, 349–361.
7 S. Donath, H. Militz and C. Mai, *Wood Sci. Technol.*, 2004, **38**, 555–566.
8 C. Mai and H. Militz, *Wood Sci. Technol.*, 2004, **37**, 339–348.
9 R. M. Rowell, *Adv. Chem. Ser.*, 1984, 175–210.
10 L. Nordstierna, S. Lande, M. Westin, O. Karlsson and I. Furo, *Holzforschung*, 2008, **62**, 709–713.
11 T. Nakagami and T. Yokota, *Mokuzai Gakkaishi*, 1983, **29**, 240–247.
12 T. Furuno and T. Goto, *Mokuzai Gakkaishi*, 1979, **25**, 488–495.
13 T. K. Timmons, J. A. Meyer and W. A. Cote, *Wood Sci.*, 1971, **4**, 13–24.
14 M. A. Ermeydan, E. Cabane, N. Gierlinger, J. Koetz and I. Burgert, *RSC Adv.*, 2014, **4**, 12981–12988.
15 E. Cabane, T. Keplinger, V. Merk, P. Hass and I. Burgert, *ChemSusChem*, 2014, **7**, 1020–1023.
16 M. A. Ermeydan, E. Cabane, A. Masic, J. Koetz and I. Burgert, *ACS Appl. Mater. Interfaces*, 2012, **4**, 5782–5789.
17 J. E. Winandy, N. M. Stark and C. M. Clemons, 5th Global Wood and Natural Fibre Composites Symposium, in Kassel, Germany, April 27–28, 2004.
18 R. W. Lenz, *Adv. Polym. Sci.*, 1993, **107**, 1–40.
19 T. Nakamura, Y. Shimizu, Y. Takimoto, T. Tsuda, Y. H. Li, T. Kiyotani, M. Teramachi, S. H. Hyon, Y. Ikada and K. Nishiya, *J. Biomed. Mater. Res.*, 1998, **42**, 475–484.
20 M. S. Reeve, S. P. Mccarthy, M. J. Downey and R. A. Gross, *Macromolecules*, 1994, **27**, 825–831.
21 R. W. Lenz and R. H. Marchessault, *Biomacromolecules*, 2004, **6**, 1–8.
22 A. M. Reed and D. K. Gilding, *Polymer*, 1981, **22**, 494–498.

23 S. Akahori and Z. Osawa, *Polym. Degrad. Stab.*, 1994, **45**, 261–265.
24 U. Raberg and J. Hafren, *Int. Biodeter. Biodegr.*, 2008, **62**, 210–213.
25 R. Sabo, L. W. Jin, N. Stark and R. E. Ibach, *Bioresources*, 2013, **8**, 3322–3335.
26 R. M. Rowell and W. D. Ellis, *Wood Fiber*, 1978, **10**, 104–111.
27 R. F. Storey and J. W. Sherman, *Macromolecules*, 2002, **35**, 1504–1512.
28 J. Libiszowski, A. Kowalski, A. Duda and S. Penczek, *Macromol. Chem. Phys.*, 2002, **203**, 1694–1701.
29 A. Duda, S. Penczek, A. Kowalski and J. Libiszowski, *Macromol. Symp.*, 2000, **153**, 41–53.
30 J. T. Wiltshire and G. G. Qiao, *Macromolecules*, 2006, **39**, 4282–4285.
31 M. Labet and W. Thielemans, *Chem. Soc. Rev.*, 2009, **38**, 3484–3504.
32 H. R. Kricheldorf, I. Kreiser-Saunders and A. Stricker, *Macromolecules*, 2000, **33**, 702–709.
33 R. F. Storey and J. W. Sherman, *Macromolecules*, 2002, **35**, 1504–1512.
34 P. V. Persson, J. Schroder, K. Wickholm, E. Hedenstrom and T. Iversen, *Macromolecules*, 2004, **37**, 5889–5893.
35 L. Liu, Y. Wang, X. Shen and Y. E. Fang, *Biopolymers*, 2005, **78**, 163–170.
36 H. Lonnberg, Q. Zhou, H. Brumer, T. T. Teeri, E. Malmstrom and A. Hult, *Biomacromolecules*, 2006, **7**, 2178–2185.
37 H. Lonnberg, K. Larsson, T. Lindstrom, A. Hult and E. Malmstrom, *ACS Appl. Mater. Interfaces*, 2011, **3**, 1426–1433.
38 R. Kusumi, Y. Teramoto and Y. Nishio, *Polymer*, 2011, **52**, 5912–5921.
39 K. Makiguchi, T. Satoh and T. Kakuchi, *Macromolecules*, 2011, **44**, 1999–2005.
40 B. Kiskan and Y. Yagci, *Polymer*, 2005, **46**, 11690–11697.
41 G. I. Mantanis, R. A. Young and R. M. Rowell, *Holzforschung*, 1994, **48**, 480–490.
42 X. H. He, L. Zhong, K. Wang, S. F. Luo and M. R. Xie, *J. Appl. Polym. Sci.*, 2010, **117**, 302–308.
43 C. A. S. Hill and G. A. Ormondroyd, *Holzforschung*, 2004, **58**, 544–547.
44 M. H. Schneider and K. I. Brebner, *Wood Sci. Technol.*, 1985, **19**, 67–73.
45 S. A. Mirmohammadi, M. Imani, H. Uyama, M. Atai, M. B. Teimouri and N. Bahri-Lale, *Polym. Int.*, 2013, **63**, 479–485.
46 A. Kavros, Y. L. Robinson and S. Rimmer, *J. Chem. Res., Synop.*, 1999, 452–453.
47 N. Gierlinger, T. Keplinger and M. Harrington, *Nat. Protoc.*, 2012, **7**, 1694–1708.
48 N. Gierlinger and M. Schwanninger, *Plant Physiol.*, 2006, **140**, 1246–1254.
49 N. Gierlinger and M. Schwanninger, *Spectrosc. – Int. J.*, 2007, **21**, 69–89.
50 H. G. M. Edwards, D. W. Farwell and D. Webster, *Spectrochim. Acta, Part A*, 1997, **53**, 2383–2392.
51 G. Kister, G. Cassanas, M. Bergounhon, D. Hoarau and M. Vert, *Polymer*, 2000, **41**, 925–932.
52 Forest Products Laboratory (U.S.), *Wood handbook: wood as an engineering material*, The Laboratory, Madison, Wis., Centennial edn, 2010.